Title
Thermal degradation and pollutant emission from waste printed circuit boards mounted with electronic components

Authors
Guo, Jie
Luo, Xiaomei
Tan, Shufei
et al.

Publication Date
2020

DOI
10.1016/j.jhazmat.2019.121038

Peer reviewed

Journal of Hazardous Materials 382 (2020) 121038

Contents lists available at ScienceDirect

Journal of Hazardous Materials

journal homepage: www.elsevier.com/locate/jhazmat

Thermal degradation and pollutant emission from waste printed circuit boards mounted with electronic components

Jie Guo[a,b], Xiaomei Luo[a], Shufei Tan[a], Oladele A. Ogunseitan[c], Zhenming Xu[a,*]

[a] School of Environmental Science and Engineering, Shanghai Jiao Tong University, 800 Dongchuan Road, Shanghai, 200240, People's Republic of China
[b] Guangzhou Key Laboratory of Environmental Catalysis and Pollution Control, School of Environmental Science and Engineering, Institute of Environmental Health and Pollution Control, Guangdong University of Technology, Guangzhou, 510006, People's Republic of China
[c] Department of Population Health and Disease Prevention & School of Social Ecology, University of California, Irvine, CA, 92697-3957, USA

GRAPHICAL ABSTRACT

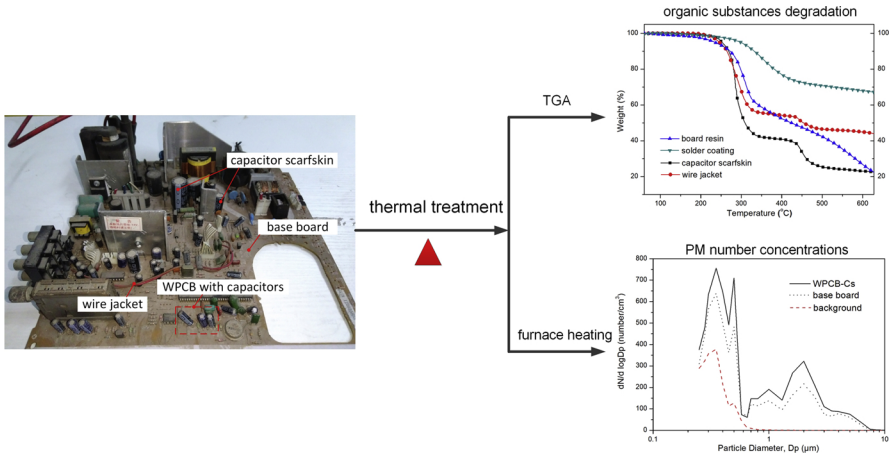

ARTICLE INFO

Editor: Deyi Hou

Keywords:
Electronic waste
Disassembly
Thermal degradation
Pollution emission

ABSTRACT

Waste printed circuit boards mounted with electronic components (WPCB-ECs) are generated from electronic waste dismantling and recycling process. Air-borne pollutants, including particulate matter (PM) and volatile organic compounds (VOCs), can be released during thermal treatment of WPCB-CEs. In this study, organic substances from WPCB-ECs were pyrolyzed by both thermo-gravimetric analysis (TGA) and in a quartz tube furnace. We discovered that board resin and solder coating were degraded in a one-stage process, whereas capacitor scarfskin and wire jacket had two degradation stages. Debromination of brominated flame retardants occurred, and HBr and phenol were the main products during TGA processing of board resin. Dehydrochlorination occurred, and HCl, benzene and toluene were detected during the pyrolysis of capacitor scarfskin. Benzene formation was found only in the first degradation stage (272–372 °C), while toluene was formed both in the two degradation stages. PM with bimodal mass size distributions at diameters of 0.45–0.5 and 4–5 μm were emitted during heating WPCB-ECs. The PM number concentrations were highest in the size ranges

* Corresponding author at: School of Environmental Science and Engineering, Shanghai Jiao Tong University, 800 Dongchuan Road, Shanghai, 200240, People's Republic of China.
E-mail address: zmxu@sjtu.edu.cn (Z. Xu).

https://doi.org/10.1016/j.jhazmat.2019.121038
Received 14 April 2019; Received in revised form 15 August 2019; Accepted 17 August 2019
Available online 18 August 2019
0304-3894/

of 0.3–0.35 μm and 1.6–2 μm. The research produced new data on pollutant emissions during thermal treatment of WPCB-ECs, and information on strategies to prevent toxic exposures that compromise the health of recyclers.

1. Introduction

Electronic waste (e-waste) is reputed to be the fastest growing category of hazardous solid waste in the world (Ogunseitan et al., 2009; Fu et al., 2018; Awasthi et al., 2019). Global generation of e-waste in 2016 was estimated to be 44.7 million metric tonnes, whereby China generated 7.2 million tonnes, ranking highest in the world (Baldé et al., 2017). In 2017, more than 71.81 million obsolete household electrical appliances, such as TV sets, refrigerators, washing machines, air conditioners and computers, were collected and dismantled in enterprises certified for e-waste recycling in China (Information System for Disposal of Waste Electrical and Electronic Equipment of the Ministry of Environmental Protection, 2019). Many kinds of secondary resources, including screen glass, metals, plastics and waste printed circuit boards (WPCB) mounted with electronic components (ECs) are processed for resource reutilization (Li et al., 2015; Turner and Filella, 2017).

Waste printed circuit boards mounted with electronic components (WPCB-ECs) are produced during reclamation of valuable materials from e-waste. The structure and composition of WPCB-ECs are complex, containing a variety of metal resources and toxic substances (Hadi et al., 2015). Previously, in order to recycle the valuable resources from WPCB-ECs, a series of primitive dismantling methods were used to remove the ECs (capacitor, resistor, chip, *etc*.) from base boards by heating over grills on a stove (Ren et al., 2014), or by using heating apparatus such as electronic soldering iron, electric blower, electronic heating furnace or rotary incinerator (An et al., 2014).

Studies of disassembly technologies for the removal of ECs from the base board have focused on using mechanical methods to replace manual disassembly (Zeng et al., 2013; Yang et al., 2009; Lee et al., 2012). (Park et al. (2015)) invented a disassembly apparatus for WPCB-ECs, in which the WPCBs was first heated with an infra-red heater in the disassembly module, then ECs were swept off from the base board by rotating steel brush rods. (Chen et al. (2013)) proposed a technology of using hot air to melt electronic components from the base boards. The best automatic heated-air disassembly efficiency was accomplished when the preheating temperature and heating source temperature were 120 °C and 260 °C, respectively, and the incubation period was 2 min. We have previously designed an automated pilot-scale equipment for disassembling ECs from WPCB (Wang et al., 2016). When the disassembling temperature, rotating speed, and incubation time were 265 °C, 10 rpm, and 8 min, respectively, the ECs and solders were easy to remove from the base boards.

Solder melting by thermal treatment with infra-red heater, hot air, or heating furnace is an important step during the removal of ECs. During the heating process, the organic materials, including board resin, plastics, brominated flame retardants (BFRs) contained in WPCB-ECs are degraded, and pollutants such as particulate matter (PM), volatile organic compounds (VOCs) (An et al., 2014; Chen et al., 2016; He et al., 2015), semi-volatile organic compounds (SVOCs) are emitted to the environment, thus causing contamination in the workshop and environmental pollution of surrounding areas (Ortuño et al., 2014a). Emission characteristics of pollutants such as polybrominated diphenyl ethers (PBDEs) (Die et al., 2019; Guo et al., 2015a, b), polybrominated dibenzo-p-dioxins/dibenzofurans (PBDD/Fs) (Xiao et al., 2016), polychlorinated dibenzo-p-dioxins/furans (PCDD/Fs), polycyclic aromatic hydrocarbons (PAHs), released from thermal treatment of WPCB have been investigated extensively (Li et al., 2018; Cai et al., 2018a, b; Duan et al., 2011; Soler et al., 2017; Ortuño et al., 2014b). However, previous studies on pollutant emission during thermal treatment have focused on the base boards of WPCB, and rarely on the pollutant emission released from ECs. In addition, the heating process of organic materials contained in WPCB-ECs generate harmful PM (Guo et al., 2019). Inhalation of PM from thermal processes can effectively deliver SVOCs, toxic metals, and brominated hydrocarbons into lung tissue, thereby deepening human exposure to these hazardous chemicals (Cormier et al., 2006). To our knowledge, there is little published information about the physical characterization of PM such as particle size distribution released from thermal treatment of WPCB-ECs.

In order to understand the emission mechanisms and clarify the pollution sources of gaseous pollutants during the disassembly of ECs from the WPCB-ECs, this study focused on the following objectives: (1) characterization of thermal degradation mechanism of organic materials contained in WPCB-ECs, including board resin, capacitor scarfskin, wire jacket, and solder coating; (2) emission characterization of PM and VOCs released from the heating process of WPCB.

2. Materials and methods

2.1. Materials

The BFRs-containing paper laminated WPCB-ECs reclaimed from obsolete cathode ray tube television sets were used as raw materials for this research (Fig. 1). Four kinds of organic materials were obtained from the WPCBs, including board resin, capacitor scarfskin, wire jacket, and solder coating. The board resin and solder coating were scratched from the surface of base board using a serrated file. The samples of capacitor scarfskin and wire jacket were cut into small pieces (2 mm × 2 mm) for the thermal test.

2.2. Thermo-gravimetric analysis (TGA)

Thermo-gravimetric analysis was performed under a helium flow of 30 mL/min with a TGA/DSC 1 (Mettler Toledo, Swiss) in a temperature range between 25 °C and 650 °C at a heating rate of 10 °C/min. The TGA was coupled with a Mass Spectrometer (GSD 320 T3, Pfeiffer Vacuum, German) by a 5 m × 150 μm/220 μm VDS tubing capillary (SGE Analytical Science, Australia). The capillary was heated to 200 °C in order to avoid the condensation of degradation products. The investigated compounds had clear molecular peaks, which enabled tracking over the investigated temperature range. Masses were scanned between $m/z = 2$ and $m/z = 300$.

Fourier transform infrared spectroscopy (FTIR) was performed with

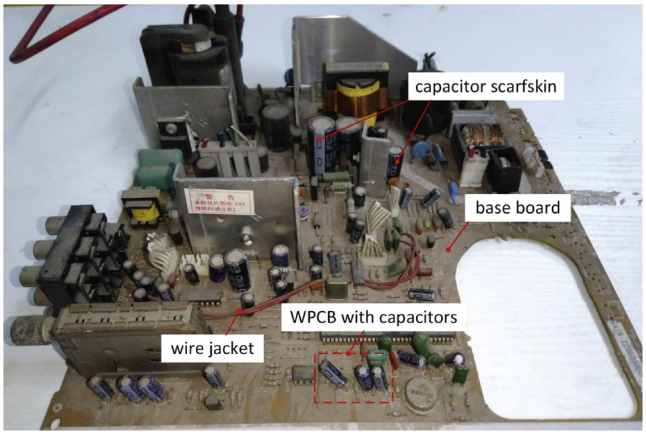

Fig. 1. WPCB-ECs dismantled from cathode ray tube television.

a Nicolet 6700 (Thermo Scientific) spectrometer to provide knowledge of functional groups. The dry sample was milled with IR grade KBr to form the KBr disk for analysis. The background spectrum of pure KBr was subtracted from that of the sample spectrum.

2.3. Quartz tube furnace heating experiments

Two kinds of samples, WPCB with capacitors (WPCB-Cs) and base board without ECs, were used for heating experiments in the quartz tube furnace. After the temperature of the furnace stabilized at 260 °C, the quartz boats containing the samples were moved into the heating zone, where they were thermally treated at isothermal conditions under an argon flow of 300 mL/min.

2.3.1. Online detection of particulate matter

The air-borne concentration and dimensions of PM after cooling were measured online by means of a laser aerosol spectrometer (Grimm Model 11-A, Germany) for 10 min. The instrument's operation is based on the principle of light scattering by a single particle inside a measurement cell. The scattered light pulse is reflected on a mirror angled to focus the light towards a detector. Then, the particles were counted, and their physical dimensions were measured by 90° scattering light detection. Grimm Model aerosol spectrometers were used for environmental measurements of PM in many studies (Cheng, 2008; Azarmia et al., 2014). A correlation (R^2) between the Grimm Aerosol Spectrometer mass concentrations and gravimetric measurements for $PM_{2.5}$ and PM_{10} were 0.94 and 0.93, respectively (Cheng, 2008). The laser aerosol spectrometer (Grimm Model 11-A, Germany) was used to measure PM characteristics every 6 s with 3 measurement modes: (1) environmental mode: PM_{10}, $PM_{2.5}$, and PM_1; (2) particulate mass size distribution; (3) particulate number size distribution. For particulate mass and number size distributions, the measured sizes ranged from 0.25 to 10 µm in 24 size channels. The sampling flow rate was 1.2 L/minute. In addition, background particle concentration inside the lab was measured for a time period of 10 min before the heating experiments.

2.3.2. Detection of volatile organic compounds

Before sampling to identify VOCs, Tenax-TA sorbent tubes (Camsco, USA) were conditioned at 320 °C for 30 min under permanent helium flow (60 mL/min). The Tenax-TA tubes were used for VOCs adsorption at the outlet of quartz tubes.

The adsorption tubes were thermally desorbed by a TD-100 multi-tube autosampler equipped with an automated re-collection system. The tubes were desorbed in splitless mode at 300 °C for 10 min with a helium flow rate of 30 mL/min and the compounds were cryogenically trapped at -10 °C into an internal focusing trap packed with 70 mg of graphitized carbon (Markes International, UK). Finally, the analytes were transferred to the chromatographic column by heating the cold trap at 280 °C for 5 min. A flow path temperature of 210 °C was used during sample analysis. The thermal desorption unit was directly connected to Gas Chromatography column through a fused silica transfer line supplied by Markes International (UK). The analyzes were performed by a GC (Trace GC Ultra, Thermo Scientific) coupled to a MS (TSQ Quantum XLS, Thermo Scientific) with an electron ionization source operating at 70 eV. Chromatographic separation was carried out by a DB-5 ms capillary column (30 m × 0.25 mm, 0.25 µm film thickness). The oven temperature program was as follows: 40 °C held for 3 min, and then ramped 5 °C/minute up to 180 °C held for 5 min, again ramped 10 °C/minute to 280 °C and held for 10 min. The constant flow rate of helium as a carrier gas was 1.5 mL/minute. A reference library (NIST/MS software version 2.0) was used to confirm the identification of the compounds by comparing the obtained element spectra with the library's spectra.

2.4. Quality assurance and quality control

All the test samples (four kinds of organic materials and WPCB-Cs) were selected from the same piece of WPCB, and the surface dust was cleaned by alcohol-soaked cotton before use. The Grimm aerosol spectrometer was calibrated before use. A gravimetric filter was installed in the aerosol spectrometer and a site-specific correction factor (C-factor = 1.0) ensured accurate response to mass concentration. Perfluorotributylamine was used to adjust the mass spectrometer calibration scale before measurement.

3. Results and discussion

3.1. TGA

Fig. 2 shows TGA and DTG thermograms of board resin, capacitor scarfskin, wire jacket, and solder coating. Values for temperature of decomposition onset (T_d), temperature with maximum rate of decomposition (T_{max}), and temperature of decomposition finish (T_f), and weight loss are presented in Table 1. The board resin and solder coating have one-stage degradation reactions, whereas the capacitor scarfskin and wire jacket have two-stage degradation reactions. The results shown in Table 1 demonstrate that the samples have different T_d values of 272 °C, 272 °C, 252 °C, and 288 °C for board resin, capacitor scarfskin, wire jacket, and solder coating, respectively.

The board resin showed a continuous process of weight loss, which is likely due to the complicated degradation process of resin matrix and additives, such as the dehydration and decarboxylation of resin matrix, and debromination of BFRs. Fig. 3a show the FTIR of board resin before

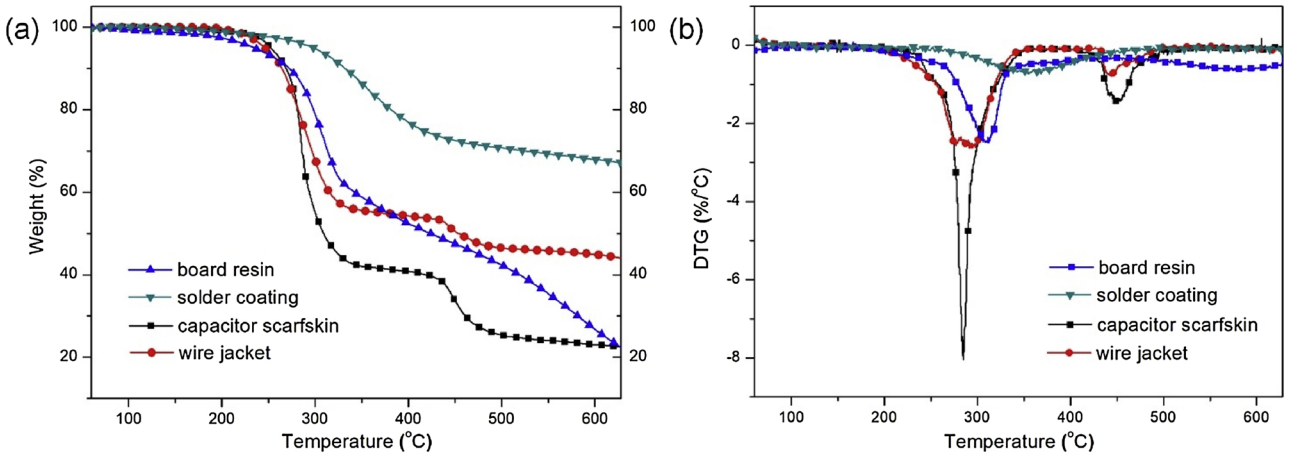

Fig. 2. TGA (a) and DTG (b) of organic substances (board resin, solder coating, capacitor scarfskin and wire jacket) from WPCB-ECs at heating rate of 10 °C/min.

Table 1
Values of temperatures (°C) and weight loss during TGA.

sample	T_d	T_{max}	T_f	weight loss (%)	residue(%)
board resin	272	309	382	77.7%	22.3%
solder coating	288	351	450	32.9%	67.1%
capacitor scarfskin	272/430	285/451	372/479	58.5%/18.9%	22.6%
wire jacket	252/421	293/443	425/500	46.7%/9.3%	44.0%

and after TGA test. The peaks at 2922 cm^{-1} and 2855 cm^{-1} were assigned to the stretching vibration of C–H, and the peaks at 1740 cm^{-1} and 1162 cm^{-1} were assigned to the stretching vibration of C═O and asymmetrical stretching vibration of C–O–C, respectively (Hadi et al., 2013; Verma et al., 2016). The peaks at 688 cm^{-1} and 579 cm^{-1} in finger print region were assigned to stretching vibration of C-Br (Zhao et al., 2006; Guo et al., 2010). The organic materials in board resin were completely degraded, a conclusion that is based on the comparison of FTIR results of board resin before and after TGA test.

The solder coating consisted mainly of acrylic ester, and the T_d of solder coating was the highest (288 °C). During the thermal degradation process, only 32.9% of weight loss was obtained, and the high char yield slowed down the degradation rate of the solder coating (Tao et al., 2018). Fig. 3b shows the FTIR of solder coating before and after TGA test. The peaks at 1735 cm^{-1} and 1407 cm^{-1} were respectively assigned to characteristic absorption peak of C═O and deformation vibration of $-CH_2$-. The peaks at 1184 cm^{-1} and 1084 cm^{-1} were assigned to the stretching vibration of C–O–C (Hadi et al., 2013; Verma et al., 2016). After thermal degradation, the carbonyl group of C═O disappeared, while many other functional groups still existed, which showed heat-resistance characteristics.

Both the capacitor scarfskin and wire jacket consisted of PVC materials, and the thermal degradation stages of the capacitor scarfskin and wire jacket were consistent with the results reported in the literature for degraded PVC (Yu et al., 2016). However, the composition and percentage of additives were different, thus leading to different weight losses during two degradation stages. For capacitor scarfskin, the weight loss was approximate 58.5% between 250 and 350 °C in the first stage. The second degradation stage began at ~420 °C with a weight loss of ~18.9%. After the second degradation step, the weight percentage of capacitor scarfskin was reduced to 22.6%.

3.2. TGA-MS analysis

Extract Ion Chromatogram (EIC) is generated by separating the ions of full mass spectra over temperature, in which data is collected only for specific *m/z* values as a function of temperature. Fig. 4 shows the EIC results of experiments designed to investigate the degradation mechanism of board resin and capacitor scarfskin, including the ion currents of selected masses during the degradation. The example of phenol is presented in Fig. 4a, whereby the *m/z* (or molecular weight) of phenol is 94, and the EIC of *m/z* 94 shows one peak between 275–380 °C. It means that the production of phenol is increasing with the increasing temperature until the peak of its production on the temperature of 324 °C whereas at higher temperature (> 324 °C), its concentrations decreases.

For the board resin, the substances of H_2O, CO_2, HBr, phenol, and methylphenols were observed between 272 and 382 °C, which were consistent with T_d and T_f temperatures of board resin during degradation (Jie et al., 2008; Li et al., 2010; Guo et al., 2014). During the degradation stage, the main source of water and CO_2 were the decomposition of resin matrix or cellulose from paper laminated WPCBs (Grause et al., 2008). BFRs are the most important additives used in board resin. The degradation of BFRs started with the formation of Br-radicals and the abstraction of hydrogen by radical transfer reactions, with HBr being the main product of the degradation of fire-retardant compounds (Ma et al., 2016). The formation of HBr started at about 270 °C and reached a peak at 310 °C. It can be assumed that the higher supply of hydrogen in the phenol or epoxy resin matrix favored the production of HBr (Hao et al., 2014). Other researchers also reported that the organic Br in the non-metallic fraction of WPCB can be converted to HBr via the pyrolysis process, with HBr and phenol being the main products (Shen et al., 2018; Kumagai et al., 2017; Terakado et al., 2011). Phenol and methylphenols were also simultaneously released during the debromination of BFRs. Other studies also found that aromatic compounds such as phenol and styrene were generated from the pyrolysis of WPCB (Evangelopoulos et al., 2015; Conesa et al., 2017; Ma and Kamo, 2018). Brominated compounds were detected from thermal decomposition of BFRs-containing products by TGA-GC/MS (Terakado et al., 2011) or pyrolysis GC/MS (Evangelopoulos et al., 2015). We also identified brominated compounds, such as bromomethane and bromophenol. The molecular weights of bromomethane (CH_3Br), bromophenol (C_6H_5BrO), 2, 4-dibromo phenol ($Br_2C_6H_3OH$) are 95, 173, and 252 g/mol, respectively. However, we did not find obvious peaks for bromomethane, bromophenol, and 2, 4-dibromo phenol. In this study, the absence of brominated compounds is likely due to the TGA-MS. The degradation products from TGA were processed through the Mass

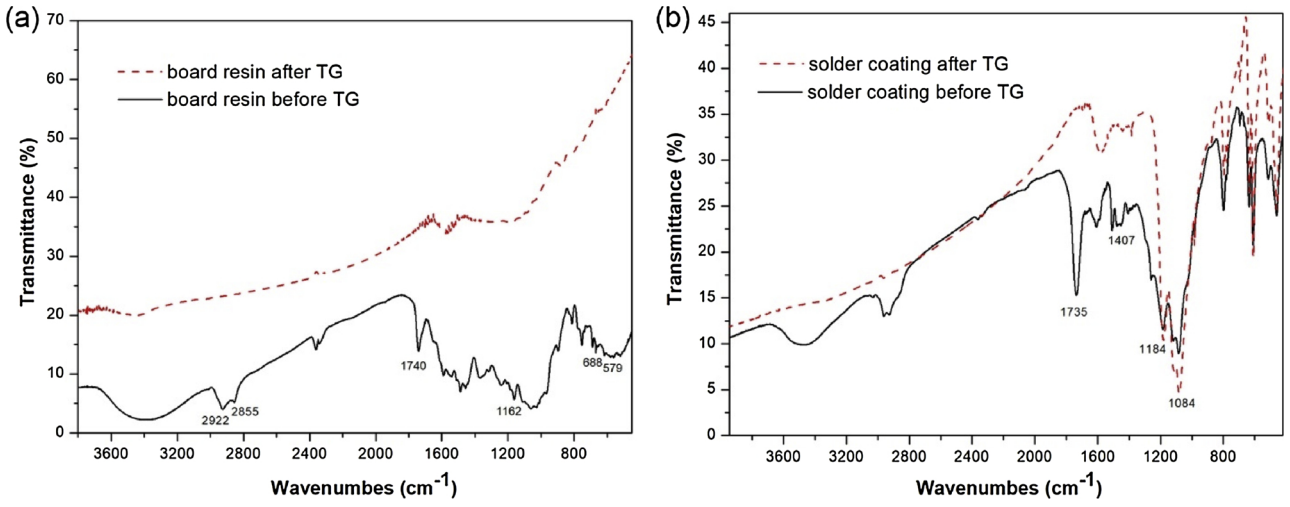

Fig. 3. FTIR spectra of board resin (a) and capacitor scarfskin (b).

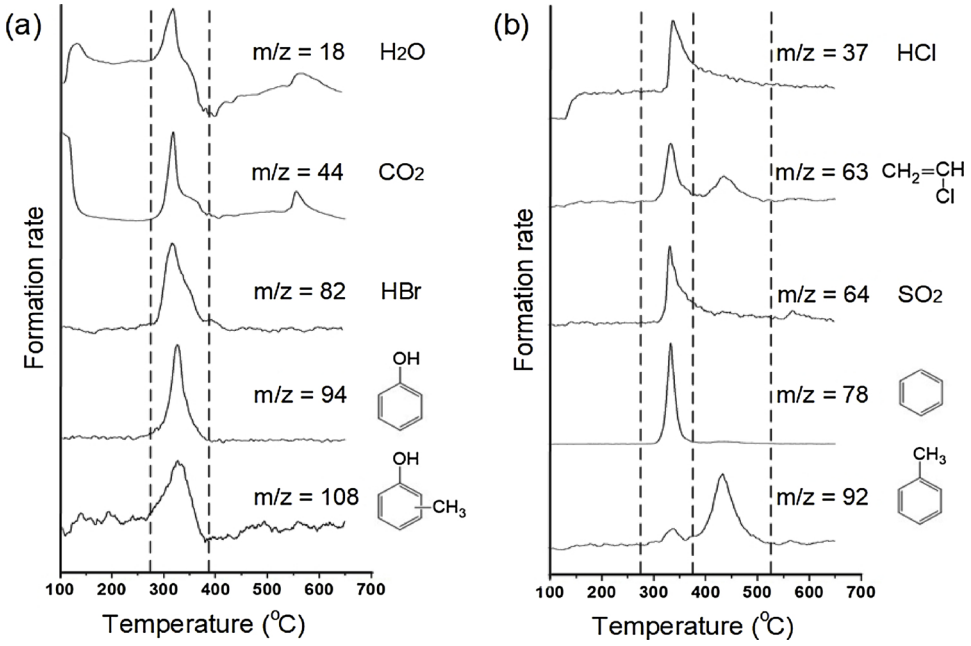

Fig. 4. Ion currents of selected masses during the degradation. (a) WPCB board resin: H_2O (m/z = 18), CO_2 (m/z = 44), HBr (m/z = 82), phenol (m/z = 94), methylphenols (m/z = 108); (b) capacitor scarfskin: HCl (m/z = 37), C_2H_3Cl (m/z = 63), SO_2 (m/z = 64), benzene (m/z = 78), toluene (m/z = 92).

Table 2
Levels of PM_{10}, $PM_{2.5}$, and PM_1 emitted from WPCB-Cs and base board (μg/m^3).

	WPCB-Cs (n = 106)	base board (n = 76)	background (n = 132)
PM_{10}	49711.3 ± 70,021.6	38046.4 ± 63,551.5	170.0 ± 11.4
RSD (%)	140.9	167.0	6.7
$PM_{2.5}$	11148.3 ± 14,270.0	7766.9 ± 11,203.2	138.7 ± 5.5
RSD (%)	128.0	144.2	4.0
PM_1	747.0 ± 590.6	562.8 ± 518.4	126.3 ± 4.5
RSD (%)	79.1	92.1	3.5

Spectrometer with VDS tubing capillary, and no Gas Chromatography was used. Brominated compounds were not detected by the MS due to the limitation of TGA-MS.

The thermal degradation of capacitor scarfskin was characterized by two distinct stages. There was a peak temperature of ~ 330 °C for HCl, C_2H_3Cl, SO_2, and benzene, which was consistent with temperature range in the first degradation stage of capacitor scarfskin in Fig. 4b. In the first stage, the main reaction was the dehydrochlorination of the PVC forming de−HCl PVC and volatile compounds (Jordan et al., 2001). The volatiles consisted mainly of HCl (m/z = 37), SO_2 (m/z = 64), benzene (m/z = 78), toluene (m/z = 92), and small amounts of vinyl chloride (m/z = 63). Other investigators have reported that HCl and benzene were the main gaseous products from PVC pyrolysis (Matsuzawa et al., 2004). However, HCl continued to be released after the first degradation stage although at decreasing levels, and HCl formation was completed at the end of the second degradation. In addition, the first and second degradation stages were also characterized by the formation of benzene and toluene, respectively. There was only 1 high peak showing the formation of benzene (m/z = 78) during the first degradation stage (285–360 °C), and the narrow peak accurately defined the beginning and end of benzene formation process in the first degradation process. In contrast to benzene, there were two peaks showing the formation of toluene (m/z = 92), a first peak and a second higher peak were observed at 330 °C and 433 °C, and the second formation process of toluene was exactly consistent with second degradation process of capacitor scarfskin. Sulfur-containing additives are used as solidifier during vulcanization process of PVC plastics, which explains the occurrence of SO_2 (m/z = 64) during the thermal degradation process (Morgan and Wilkie, 2014).

3.3. Heating Experiments in the quartz tube furnace

Four kinds of organic materials (board resin, solder coating, capacitor scarfskin, and wire jacket) were used for TGA-MS experiment, while only WPCB-Cs with board resin and capacitor scarfskin were used for furnace heating experiments. The reasons were as follows: (1) Both capacitor scarfskin and wire jacket consisted of PVC materials with similar thermal degradation processes, and the weight loss percent of capacitor scarfskin was higher than that of wire jacket (Fig. 2 and Table 1). So capacitor scarfskin in WPCB-Cs was chosen for the furnace heating experiments. (2) The solder coating possessed the best thermal stability, with highest T_d and lowest weight loss (Fig. 2 and Table 1). The T_d for solder coating was 288 °C, which was higher than 260 °C in furnace heating experiments. In addition, only a thin layer of solder coating was coated on the base board. Therefore, the degradation of solder coating was not considered when doing furnace experiments.

3.3.1. Levels of PM_{10}, $PM_{2.5}$, and PM_1

The average levels of PM_{10}, $PM_{2.5}$, and PM_1 emitted from WPCB-Cs, base board, and the background are reported in Table 2. Average concentrations of PM_{10} and $PM_{2.5}$ emitted from PCBs and base board were 56 to 292 times higher than the background ambient level. High concentrations of PM were released from the heating process of WPCB-Cs and base board compared to the background concentrations. The highest average mass concentrations of PM_{10}, $PM_{2.5}$, and PM_1 were observed from the heating process of WPCB-Cs. This may be caused by thermal degradation of resin matrix of base board and the PVC materials of capacitor scarfskin.

The ratios of $PM_{2.5}/PM_{10}$ from WPCB-Cs and base board were 0.224 and 0.204, respectively, indicating that the heating process of WPCB can generate high proportions of coarse particles. The proportions of PM_1:$PM_{2.5}$:PM_{10} emitted from WPCB-Cs and base board were similar, with the values of 1:14.9:66.5 and 1:13.8:67.6, which were different from the proportion of PM background (1:1.09:1.35).

3.3.2. Number and mass concentrations of emitted PM

Fig. 5 shows the distribution of particulate mass concentrations and

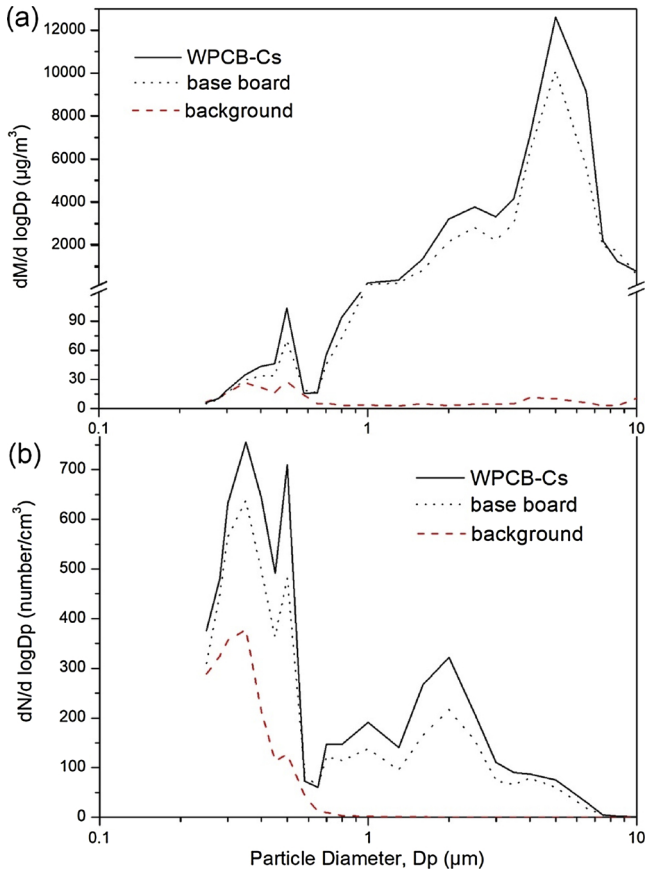

Fig. 5. The particulate mass (a) and number (b) size distributions during thermal treatment of WPCB.

size distributions for background, base board, and WPCB-Cs. Overall, an obviously increase in the number and mass concentrations of emitted fumes from WPCB-Cs and base board compared to the background. For PM emitted from WPCB-Cs and base board, bimodal mass size distributions were found at diameters of 0.45-0.5 μm and 4–5 μm, respectively. Particulates with diameters larger than 0.7 μm predominated. The total mass concentrations of emitted fumes from WPCB-Cs and base board were 50.1 and 38.4 mg/m^3, respectively. The highest mass concentrations were found to correspond to particles with 4–5 μm size distribution, with mass concentrations of 12.6 and 10.1 mg/m^3, respectively.

Meanwhile, the concentration and size distribution indicated that the counts of particle in the size ranges of 0.3-0.35 μm and 1.6–2 μm had a sharp increase in number concentration. The total number concentrations of emitted fumes from WPCB-Cs and base board were 6046 and 4762 particles per cm^3, respectively. The results presented in Fig. 5b show that particles smaller than 0.6 μm predominated. The highest concentration of PM correspond to the particle with 0.3-0.35 μm size range, with concentrations of 756 and 638 particles per cm^3. Although fine particles between 0.3 μm and 0.35 μm dominated, their contributions to PM_1 were small, representing 5.0–5.5 weight percentage of PM_1 emitted from WPCB-Cs and base board.

The distribution of particulate mass and concentrations depended on the materials and heating parameters. The composition and particle size of the materials are expected to influence the PM emission during thermal treating or open burning processes. Heating parameters, such as gas atmosphere, heating methods (thermal treatment, open burning, or pyrolysis), temperature, the turbulence of gas, always have effects on the particle formation and particulate distribution. The PM formation and particle distribution are complicated consequences of the heating process. In Li et al.'s study (Li et al., 2018), small pieces of waste printed circuit board (830–1700 μm) were heated (300 °C for 150 min) or open burned (800–1350 °C for 3 min) under desiccant air atmosphere for modeling experiments in a chamber. The distributions of PM in Li et al.'s study (Li et al., 2018) were detected by a Micro-Orifice Uniform Deposit Impactor (MOUDI). In our study, the WPCB-Cs were heated at 260 °C under argon atmosphere in a quartz tube. The heating methods are different. In addition, the distribution of PM was based on an online laser aerosol spectrometer (Grimm Model). Therefore, the difference between the two studies was reasonable and expected.

The source of PM was multi-component vapor-gaseous mixture, formed by evaporation of water, CO_2, VOCs, and SVOCs when the organic compounds in WPCB-Cs were heated at a high temperatures. Four mechanisms are responsible for the formation of PM: condensation, coagulation, adsorption SVOCs onto existing solid particles, and dissolution of soluble gases in particles or droplets (USEPA, 2004). When vapor is cooled by the water-cooling process, new particles may be formed by nucleation from gas phase materials, and the low-equilibrium vapor pressure gas molecules condense on a particle. Fine particles can also be produced by coagulation (two particles combining to form one) or by condensation (low-equilibrium vapor pressure gas molecules condensing on a particle). As the particle size increases, the rate of growth decreases and particles accumulated in the accumulation mode size range (0.1–2 μm). The accumulation-mode particles with a hydroscopic component, grow into droplets as the relative humidity increases. Meanwhile, large variety of organic compounds condense to liquid oil, in which the SVOCs dissolve. The accumulation mode and the coarse mode (2–10 μm) overlap in the region between 1 μm and 3 μm. In this region, there was an obvious peak in the concentration of PM (Fig. 5b).

3.3.3. VOCs emission from board resin

The board resin dominated the weight of organic materials contained in the WPCB-ECs, and the VOCs emission from base board was detected using sorbent adsorption and thermal desorption & GC–MS.

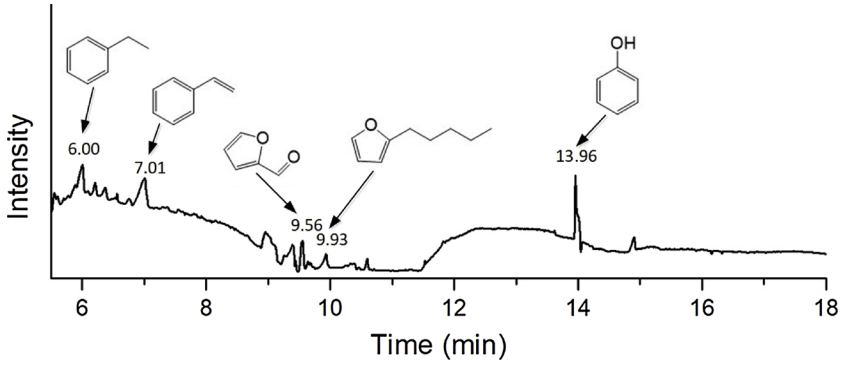

Fig. 6. Total ion chromatogram (TIC) of VOCs released from isothermal pyrolysis of board resin.

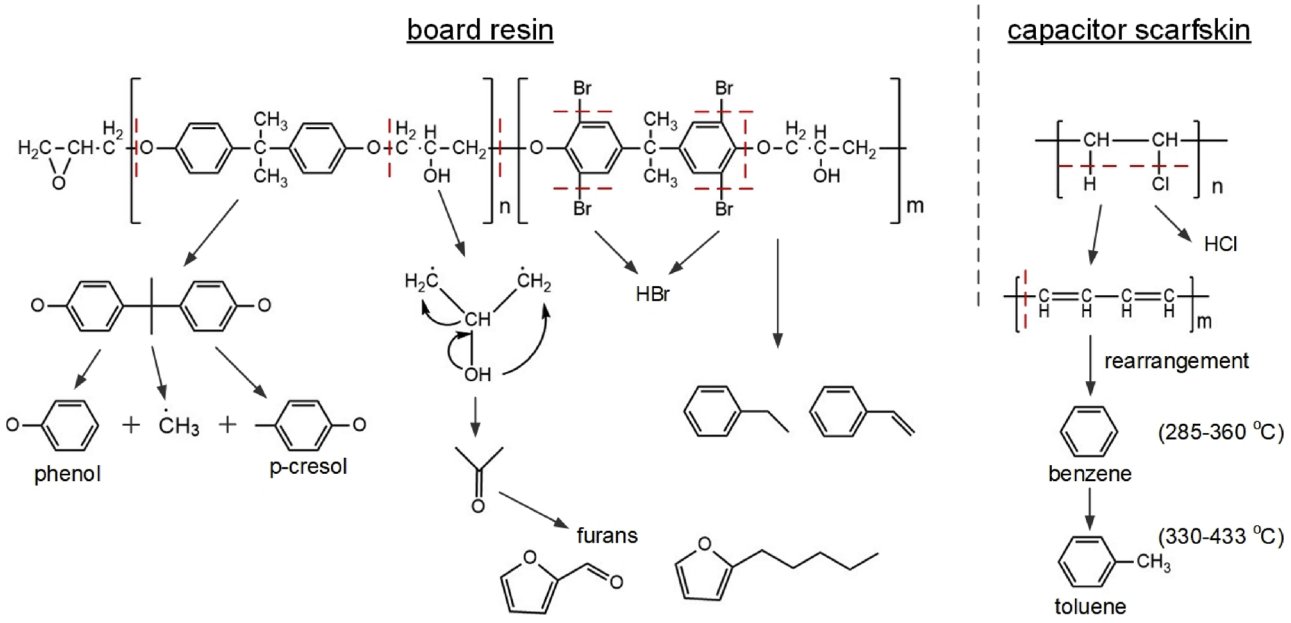

Fig. 7. Thermal degradation pathways of WPCB-ECs.

The total ion chromatogram (TIC) of VOCs released from board resin at isothermal pyrolysis condition (260 °C) are shown in Fig. 6. Dehydration and the production of aromatic compounds and furans were observed at different retention time (RT). Aromatic substances such as ethylbenzene (RT = 6.00), styrene (RT = 7.01), and phenol (RT = 13.96) were found in the TIC. Other toxic furans such as furan-2-carboxaldehyde (RT = 9.56) and 2-pentylfuran (RT = 9.93) were also detected. The additional mass spectra are shown in Fig. S1.

The degradation mechanisms and pathways of organic substances contained in WPCB-ECs are complex. The board resin accounted for the most weight of organic materials, and a wide range of aromatics, nonaromatic ring-retaining and ring-opening products were generated due to the chain scission processes of resin matrix and molecular rearrangement of radicals (·Br, ·Cl, ·CH_3, *etc.*) or precursors. A possible degradation mechanism of board resin and capacitor scarfskin is shown in Fig. 7. HBr and HCl are constantly released in high concentrations from board resin, BFRs, and PVC materials. Aromatic compounds such as phenol and benzene are the main organic products from WPCB-ECs degradation. In addition, furans and dioxin precursors can also be generated (Barontini and Cozzani, 2006). Kumagai et al., (Kumagai et al., 2017) investigated the debromination of brominated phenols in the presence of CaO through charge transfer, and phenol was produced from thermal degradation (mainly below 300 °C) of phenol resin paper-laminated WPCB. Evangelopoulos et al., (Evangelopoulos et al., 2015) also found that aromatic compounds such as styrene, methylstyrene, phenol, and benzene were produced due to board resin's decomposition.

4. Conclusions

This research investigated the thermal degradation process of organic substances contained in WPCB-ECs in a quartz tube furnace and thermos-gravimetric analysis. Four kinds of organic substances, including board resin, capacitor scarfskin, wire jacket, and solder coating from WPCB-CEs, were used for TGA. The results of TGA-MS, FTIR, online detection of PM, and sorbent adsorption of VOCs showed that HBr and phenol were the main degradation products from board resin, while HCl, benzene, and toluene were main products from heating of capacitor scarfskin. The emission features of PM, particulate mass/number size distributions from WPCB-Cs and base board were compared and analyzed. The results showed that thermal treatment of organic substances contained in board resin and plastics could lead to PM and VOCs pollution. Therefore, it is important to monitor the environment in which WPCB-ECs are dismantled and to provide e-waste workers with personal protective equipment to reduce toxic exposures.

Declaration of Competing Interest

The authors declare they have no actual or potential competing financial interests.

Acknowledgments

This work was supported by the National Natural Science Foundation of China (41877468, 51778360), Guangzhou Key Laboratory of Environmental Catalysis and Pollution Control (GKLECPC-07), Natural Science Foundation of Shanghai (18ZR1418200), and Shanghai Pujiang Program (18PJD022).

Appendix A. Supplementary data

Supplementary material related to this article can be found, in the online version, at doi:https://doi.org/10.1016/j.jhazmat.2019.121038.

References

Ogunseitan, O.A., Schoenung, J.M., Saphores, J.D., Shapiro, A.A., 2009. The electronics revolution: from e-wonderland to e-wasteland. Science 326, 670–671.
Fu, J., Zhang, H., Zhang, A., Jiang, G., 2018. E-waste recycling in China: a challenging field. Environ. Sci. Technol. 52, 6727–6728.
Awasthi, A.K., Li, J., Koh, L., Ogunseitan, O.A., 2019. Circuit economy and electronic waste. Nat. Electron. 2, 86–89.
Baldé, C.P., Forti, V., Gray, V., Kuehr, R., Stegmann, P., 2017. The Global e-waste monitor-2017, United Nations University (UNU). International Telecommunication Union (ITU) & International Solid Waste Association (ISWA), Bonn/Geneva/Vienna.
Information System for Disposal of Waste Electrical and Electronic Equipment of the Ministry of Environmental Protection Information System for Disposal of Waste Electrical and Electronic Equipment of the Ministry of Environmental Protection, China (accessed 9 April 2019). http://weee.mepscc.cn/Index.do?method=list&newsType=4.
Li, J., Zeng, X., Chen, M., Ogunseitan, O.A., Stevels, A., 2015. Control-Alt-Delete: rebooting solutions for the e-waste problem. Environ. Sci. Technol. 49, 7095–7108.
Turner, A., Filella, M., 2017. Bromine in plastic consumer products-Evidence for the widespread recycling of electronic waste. Sci. Total Environ. 601-602, 374–379.
Hadi, P., Xu, M., Lin, C.S.K., Hui, C., McKay, G., 2015. Waste printed circuit board recycling techniques and product utilization. J. Hazard. Mater. 283, 234–243.
Ren, Z., Xiao, X., Chen, D., Bi, X., Huang, B., Liu, M., Hu, J., Peng, P.A., Sheng, G., Fu, J.,

2014. Halogenated organic pollutants in particulate matters emitted during recycling of waste printed circuit boards in a typical e-waste workshop of Southern China. Chemosphere 94, 143–150.
An, T., Huang, Y., Li, G., He, Z., Chen, J., Zhang, C., 2014. Pollution profiles and health risk assessment of VOCs emitted during e-waste dismantling processes associated with different dismantling methods. Environ. Int. 73, 186–194.
Zeng, X., Li, J., Xie, H., Liu, L., 2013. A novel dismantling process of waste printed circuit boards using water-soluble ionic liquid. Chemosphere 93, 1288–1294.
Yang, J., Xiang, D., Wang, J., Duan, G., Zhang, H., 2009. Removal force models for component disassembly from waste printed circuit board. Resour. Conserv. Recy. 53, 448–454.
Lee, J., Kim, Y., Lee, J., 2012. Disassembly and physical separation of electric/electronic components layered in printed circuit boards (PCB). J. Hazard. Mater. 241-242, 387–394.
Park, S., Kim, S., Han, Y., Park, J., 2015. Apparatus for electronic component disassembly from printed circuit board assembly in e-wastes. Int. J. Miner. Process. 144, 11–15.
Chen, M., Wang, J., Chen, H., Ogunseitan, O.A., Zhang, M., Zang, H., Hu, J., 2013. Electronic waste disassembly with industrial waste heat. Environ. Sci. Technol. 47, 12409–12416.
Wang, J., Guo, J., Xu, Z., 2016. An environmentally friendly technology of disassembling electronic components from waste printed circuit boards. Waste Manage. 53, 218–224.
Chen, J., Zhang, D., Li, G., An, T., Fu, J., 2016. The health risk attenuation by simultaneous elimination of atmospheric VOCs and POPs from an e-waste dismantling workshop by an integrated de-dusting with decontamination technique. Chem. Eng. J. 301, 299–305.
He, Z., Li, G., Chen, J., Huang, Y., An, T., Zhang, C., 2015. Pollution characteristics and health risk assessment of volatile organic compounds emitted from different plastic solid waste recycling workshops. Environ. Int. 77, 85–94.
Ortuño, N., Conesa, J.A., Moltó, J., Font, R., 2014a. Pollutant emissions during pyrolysis and combustion of waste printed circuit boards, before and after metal removal. Sci. Total Environ. 499, 27–35.
Die, Q., Nie, Z., Huang, Q., Yang, Y., Fang, Y., Yang, J., He, J., 2019. Concentrations and occupational exposure assessment of polybrominated diphenyl ethers in modern Chinese e-waste dismantling workshops. Chemosphere 214, 379–388.
Guo, J., Zhang, R., Xu, Z., 2015a. PBDEs Emission from waste printed wiring boards during thermal process. Environ. Sci. Technol. 49, 2716–2723.
Guo, J., Lin, K., Deng, J., Fu, X., Xu, Z., 2015b. Polybrominated diphenyl ethers in indoor air during waste TV recycling process. J. Hazard. Mater. 283, 439–446.
Xiao, X., Hu, J., Peng, P.A., Chen, D., Bi, X., 2016. Characterization of polybrominated dibenzo-p-dioxins and dibenzo-furans (PBDDs/Fs) in environmental matrices from an intensive electronic waste recycling site, South China. Environ. Pollut. 212, 464–471.
Li, T., Zhou, J., Wu, C., Bao, L., Shi, L., Zeng, E.Y., 2018. Characteristics of polybrominated diphenyl ethers released from thermal treatment and open burning of e-waste. Environ. Sci. Technol. 52, 4650–4657.
Cai, C., Yu, S., Liu, Y., Tao, S., Liu, W., 2018a. PBDE emission from e-wastes during the pyrolytic process: emission factor, compositional profile, size distribution, and gas-particle partitioning. Environ. Pollut. 235, 419–428.
Cai, C., Yu, S., Li, X., Liu, Y., Tao, S., Liu, W., 2018b. Emission characteristics of polycyclic aromatic hydrocarbons from pyrolytic processing during dismantling of electronic wastes. J. Hazard. Mater. 351, 270–276.
Duan, H., Li, J., Liu, Y., Yamazaki, N., Jiang, W., 2011. Characterization and inventory of PCDD/Fs and PBDD/Fs emissions from the incineration of waste printed circuit board. Environ. Sci. Technol. 45, 6322–6328.
Soler, A., Conesa, J.A., Ortuño, N., 2017. Emissions of brominated compounds and polycyclic aromatic hydrocarbons during pyrolysis of e-waste debrominated in subcritical water. Chemosphere 186, 167–176.
Ortuño, N., Moltó, J., Conesa, J.A., Font, R., 2014b. Formation of brominated pollutants during the pyrolysis and combustion of tetrabromobisphenol A at different temperatures. Environ. Pollut. 191, 31–37.
Guo, J., Ji, A., Wang, J., Ogunseitan, O.A., Xu, Z., 2019. Emission characteristics and exposure assessment of particulate matter and polybrominated diphenyl ethers (PBDEs) from waste printed circuit boards de-soldering. Sci. Total Environ. 662, 530–536.
Cormier, S.A., Lomnicki, S., Backes, W., Dellinger, B., 2006. Origin and health impacts of emissions of toxic by-products and fine particles from combustion and thermal treatment of hazardous wastes and materials. Environ. Health Persp. 114, 810–817.
Cheng, Y.-H., 2008. Comparison of the TSI Model 8520 and Grimm Series 1.108 portable aerosol instruments used to monitor particulate matter in an iron foundry. J. Occup. Environ. Hyg. 5, 157–168.
Azarmia, F., Kumarab, P., Mulheron, M., 2014. The exposure to coarse, fine and ultrafine particle emissions from concrete mixing, drilling and cutting activities. J. Hazard. Mater. 279, 268–279.
Hadi, P., Gao, P., Barford, J.P., McKay, G., 2013. Novel application of the nonmetallic fraction of the recycled printed circuit boards as a toxic heavy metal adsorbent. J. Hazard. Mater. 252–253, 166–170.
Verma, H.R., Singh, K.K., Mankhand, T.R., 2016. Dissolution and separation of brominated epoxy resin of waste printed circuit boards by using di-methyl formamide. J. Clean. Prod. 139, 586–596.
Zhao, M., Li, J., Wen, X., 2006. Experimental research of pyrolysis contamination during crushing of fire-retardant phenolic-resin-based printed wiring boards. Min. & Metall. 15, 78–83 (in Chinese).
Guo, Q., Yue, X., Wang, M., Liu, Y., 2010. Pyrolysis of scrap printed circuit board plastic particles in a fluidized bed. Powder Technol. 198, 422–428.
Tao, X., Duan, H., Dong, W., Wang, X., Yang, S., 2018. Synthesis of an acrylate constructed by phosphaphenanthrene and triazine-trione and its application in intrinsic flame retardant vinyl ester resin. Polym. Degrad. Stabil. 154, 285–294.
Yu, J., Sun, L., Ma, C., Qiao, Y., Yao, H., 2016. Thermal degradation of PVC: a review. Waste Manage. 48, 300–314.
Jie, G., Ying-Shun, L., Mai-Xi, L., 2008. Product characterization of waste printed circuit board by pyrolysis. J. Anal. Appl. Pyrol. 83, 185–189.
Li, J., Duan, H., Yu, K., Liu, L., Wang, S., 2010. Characteristic of low-temperature pyrolysis of printed circuit boards subjected to various atmosphere. Resour. Conserv. Recy. 54, 810–815.
Guo, X., Qin, F.G.F., Yang, X., Jiang, R., 2014. Study on low-temperature pyrolysis of large-size printed circuit boards. J. Anal. Appl. Pyrol. 105, 151–156.
Grause, G., Furusawa, M., Okuwaki, A., Yoshioka, T., 2008. Pyrolysis of tetrabromobisphenol-A containing paper laminated printed circuit boards. Chemosphere 71, 872–878.
Ma, C., Yu, J., Wang, B., Song, Z., Xiang, J., Hu, S., Su, S., Sun, L., 2016. Chemical recycling of brominated flame retarded plastics from e-waste for clean fuels production: a review. Renew. Sust. Energ. Rev. 61, 433–450.
Hao, J., Wang, H., Chen, S., Cai, B., Ge, L., Xia, W., 2014. Pyrolysis characteristics of the mixture of printed circuit board scraps and coal powder. Waste Manage. 34, 1763–1769.
Shen, Y., Chen, X., Ge, X., Chen, M., 2018. Thermochemical treatment of non-metallic residues from waste printed circuit board: pyrolysis vs. Combustion. J. Clean. Prod. 176, 1045–1053.
Kumagai, S., Grause, G., Kameda, T., Yoshioka, T., 2017. Thermal decomposition of tetrabromobisphenol-A containing printed circuit boards in the presence of calcium hydroxide. J. Mater. Cycles. Waste 19, 282–293.
Terakado, O., Ohhashi, R., Hirasawa, M., 2011. Thermal degradation study of tetrabromobisphenol A under the presence metal oxide: comparison of bromine fixation ability. J. Anal. Appl. Pyrol. 91, 303–309.
Evangelopoulos, P., Kantarelis, E., Yang, W., 2015. Investigation of the thermal decomposition of printed circuit boards (PCBs) via thermogravimetric analysis (TGA) and analytical pyrolysis (Py-GC/MS). J. Anal. Appl. Pyrol. 115, 337–343.
Conesa, J.A., Ortuño, N., Zielinska, A., 2017. Thermal decomposition of three types of copper clad laminates considering the influence of an iron-clay catalyst in the production of pollutants. J. Anal. Appl. Pyrol. 126, 62–69.
Ma, C., Kamo, T., 2018. Two-stage catalytic pyrolysis and debromination of printed circuit boards: effect of zero-valent Fe and Ni metals. J. Anal. Appl. Pyrol. 134, 614–620.
Jordan, K.J., Suib, S.L., Koberstein, J.T., 2001. Determination of the degradation mechanism from the kinetic parameters of dehydrochlorinated poly(vinyl chloride) decomposition. J. Phys. Chem. B 105, 3174–3181.
Matsuzawa, Y., Ayabe, M., Nishino, J., Kubota, N., Motegi, M., 2004. Evaluation of char fuel ratio in municipal pyrolysis waste. Fuel 83, 1675–1687.
Morgan, A.B., Wilkie, C.A., 2014. The Non-Halogenated Flame Retardant Handbook. Scrivener Publishing, Beverly, MA, USA.
USEPA, 2004. Air Quality Criteria for Particulate Matter (EPA/600/P-99/002aF), Research Triangle Park, NC. (Accessed 9 April 2019. https://cfpub.epa.gov/si/si_public_record_report.cfm?Lab=NCEA&dirEntryId=87903.
Barontini, F., Cozzani, V., 2006. Formation of hydrogen bromide and organobrominated compounds in the thermal degradation of electronic boards. J. Anal. Appl. Pyrol. 77, 41–55.